Catalysis Science & Technology

Accepted Manuscript

ROYAL SOCIETY OF CHEMISTRY

www.rsc.org/catalysis

Catalysis Science & Technology RSCPublishing

Paper

Promotion Effect of Fe in Mordenite Zeolite on Carbonylation of Dimethyl Ether to Methyl Acetate

Cite this: DOI: 10.1039/x0xx00000x

Hui Zhou[a,b,c], Wenliang Zhu[a,b], Lei Shi[a,b], Hongchao Liu[a,b], Shiping Liu[a,b,c], Shutao Xu[a,b], Youming Ni[a,b], Yong Liu[a,b], Lina, Li[a,b,c], Zhongmin Liu[*a,b]

Received 00th January 2014,
Accepted 00th January 2014

DOI: 10.1039/x0xx00000x

www.rsc.org/

A series of Fe-modified mordenite zeolite samples were synthesized by a template-free method and employed in dimethyl ether (DME) carbonylation reaction for the production of methyl acetate (MAc). XRD, UV-Vis, and UV-Raman characterization studies proved that Fe atoms have been introduced into the mordenite zeolite framework by partial substitution of Al atoms, which led to an evident change of activity and MAc selectivity. With the increase of iron content (as metal) from 0.0 to 3.6wt%, DME conversion first increased and then decreased. MAc selectivity and catalyst stability were enhanced for all Fe-modified samples. TG and GC-MS analysis of deactivated catalysts showed that the amount of coke retained in catalysts decreased as the iron content in zeolites increased. The enhancement effects were expounded in terms of the decrease of acid strength and acid density in 12MR channels of mordenite after introduction of Fe, resulting in reduction of carbon deposition.

1. Introduction

The carbonylation reaction of dimethyl ether (DME) to methyl acetate (MAc) has triggered wide research interest[1-8] because the product of MAc hydrogenation, ethanol, can be applied in wide fields.[9-13] This novel production process of ethanol is highly competitive compared with the traditional processes of hydration of ethylene and fermentation of sugars and corns because the DME can be readily derived from synthesis gas ($CO + H_2$, syngas).[14] The copper-based catalyst used in the hydrogenation reaction has been in commercial operations. The major challenge during the research of this novel process is to develop effective heterogeneous zeolite catalysts for DME carbonylation reaction with excellent performance in terms of activity, selectivity and stability.

In 1984, Fujimoto et.al first reported results from studies of vapor carbonylation of methanol with heterogeneous zeolite catalysts. They found that HY and HMOR zeolite catalysts demonstrated some carbonylation activity with low MAc selectivity.[1] Iglesia and his co-workers[2-4] initiated detailed researches on DME carbonylation to MAc with zeolite catalysts (H-MOR, H-FER and H-ZSM5) and reported that HMOR zeolite could catalyze DME carbonylation reaction to MAc at low temperatures (423–463 K) with remarkable selectivity (>99% MAc selectivity), but the MAc productivity was below the expected commercial target. Also, HMOR catalyst with 8MR and 12MR channels had the highest MAc synthesis rate and the controlling step of carbonylation reaction (3) occurred in the 8MR channels. Quantum-chemical calculation results[5] showed that only T3-O33 positions in the 8MR channels of mordenite were selective for acetyl generation. Highly selective property of HMOR catalyst was not only due to the size of 8MR channel but also to the unusual orientation of methoxy group in the relation to the 8MR channel (parallel to the cylinder axis)[5]. The in-situ solid-state NMR spectroscopy studies also confirmed that important surface acetyl immediate species could only be identified in the 8MR channels, not on the active sites in 12MR channels, where the active sites favored the formation of hydrocarbons.[6] According to the present understanding about this reaction, catalyst stability, one of the important factors for industrial application, can be enhanced by occupying or removing the acid sites in 12MR channels of mordenite, where the formation of high molecular weight hydrocarbons like aromatic will occur, resulting in the deactivation of catalyst. Shen et.al reported the related work on development of improved zeolite catalysts for DME carbonylation by pre-adsorption of pyridine[7] or selective dealumination of H-mordenite zeolite,[8] and obtained considerable improvement in the performance of MOR catalyst for DME carbonylation reaction.

Introduction of metal atoms in the framework or extra-framework of zeolites is an important route to change physiochemical properties of zeolites and thus improve their performance in reactions.[15] Brian Ellis et.al reported that H-MOR and Cu-MOR were active and selective for methanol vapor phase carbonylation reaction under moderate operating conditions.[16] For DME carbonylation reaction, introduction of Cu and Ag by ion exchange to replace counter ion H was reported in publications and patents.[17, 18] FTIR and solid state NMR studies proved that Cu-H-MOR had two neighboring sites, bridged hydroxyl and neighboring Cu^+, and contributed to the formation of MAc. Besides the activity of catalysts, the

product selectivity and stability of catalyst are the major challenge for the development of the DME carbonylation reaction. Zeolites containing Fe in frameworks showed excellent performances in many catalysis reactions.[19, 20] Here, we reported the results from studies of DME carbonylation with Fe-modified mordenites which were synthesized by a template-free hydrothermal method. The physical structure of Fe^{3+} framework-substituted mordenites were characterized by XRD, UV-Vis, UV-Raman and N_2-adsorption, the acid sites strength and density were characterized by ^{31}P MAS NMR and FTIR spectra after adsorption of base probe molecules.

2. Experiment

2.1 Catalysts preparation

Iron nitrate [$Fe(NO_3)_3 \cdot 9H_2O$], sodiumaluminate [$NaAlO_2$], and silica sol (30% Si content) were used as initial Fe, Al, Si sources, respectively. Si/Al in sol was 10 and desired Fe contents were 0.0 wt%, 0.9 wt%, and 1.8 wt%, 3.6wt% in the proposed product $Na_{(x+y)}Fe_xAl_ySi_zO_{2(x+y+z)}$, estimated by the formula:

$$Fewt\% = \frac{Fewt}{Fewt + Alwt + Owt + Siwt + Nawt} \times 100\%$$

The gel was sealed in a Teflon beaker and heated at 453 K with agitation. After crystallization for 20 h, solid product was filtered and washed with de-ionized water. The products were labeled as FeNaMOR-0, FeNaMOR-0.9, FeNaMOR-1.8 and FeNaMOR-3.6. HMOR samples were obtained from NaMOR samples by ion exchange. The NaMOR sample was dispersed in NH_4NO_3 aqueous solution (1 mol/L, 1gsolid: 10mLsolution) at 353 K for 2 h and then filtered and washed with de-ionized water. After repeating ion exchange three times, the resulting solid was dried at 393 K overnight in ambient air and then calcined in flowing dry air (20mL/min/g) at 673 K for 8 h. The as-prepared catalysts were labeled as FeHMOR-0, FeHMOR-0.9, FeHMOR-1.8 and FeHMOR-3.6, respectively.

2.2. Catalysts characterization

X-Ray powder diffractograms were recorded at room temperature using Cu Kα radiation (PANalytical X' Pert Pro diffractometer).

Iron content was obtained by XRF analysis (PANalytical AXIOS).

UV–Vis reflectance spectra were collected on a Varian Cary spectrophotometer with a powdered Fe-containing sample and $BaSO_4$ was used as a reference.

IR spectra in the framework vibration region were recorded with a spectral resolution of 4 cm^{-1} using KBr technique (weight ratio of sample to KBr, 1:100).

UV-Raman spectra were recorded on a DL-2 Raman spectrometer, with a collection time of 300 s. A 244 nm line of a LEXEL laser was used as the excitation sources. The laser power at the sample was less than 5 mW. The spectrometer for Raman scattering was an Acton triple monochromator. The Prinston CCD detector was used to collect the spectra.

Nitrogen sorption experiments were performed at 77 K on Micromeritics ASAP-2020 system with a static measurement mode. Tested samples were degassed at 623 K for 4 h prior to each measurement. BET surface areas were calculated by the standard multi-point method, and pore volume was determined by N_2 adsorption at a relative pressure of 0.98.

The ^{31}P MAS NMR spectra were recorded on Bruker AvanceIII 600 spectrometer using a 4 mm probe. The ^{31}P MAS NMR spectra were acquired with high-power decoupling, a repetition time of 4s, a π/4 pulse length of 2 μs and a spinning speed of 12 kHz. The ^{31}P NMR chemical shifts were referenced to 85% H_3PO_4. In a typical adsorption experiment, the FeHMOR zeolite was subjected to dehydration before the adsorption of trimethylphosphine oxide (TMPO) probe molecule. The temperature of the sample increased to 673 K at a rate of 2 K/min and maintained for 8 h and then cooled to the room temperature. After the TMPO dissolved in the CH_2Cl_2 was added into the sample in the three-necked round-bottomed flask in N_2 glovebox, the sample was stirred overnight in N_2 atmosphere. The removal of CH_2Cl_2 was conducted at about 323 K. The sealed sample vessel was further subjected to a baking treatment at 453 K for 8 h to ensure a uniform adsorption of TMPO in the channels of mordenite. Then TMPO crystal that did not reacted with the sample was evacuated at 453 K.

Fourier transform infrared (FT-IR) spectra after pyridine adsorption were obtained on a Bruker tensor 27 instrument with a resolution of 4 cm^{-1}. Samples were pressed into a self-supporting wafer (R=0.65 cm, 15 mg) and evacuated (2×10^{-2} Pa) in the IR cell at 673 K for 1 h prior to each measurement. Adsorption of pyridine was conducted at 573 K for 15 min to ensure a saturated loading and then evacuated for 1h prior to acquisition of IR spectra. Densities of Brønsted and Lewis acid sites were calculated from the IA values of difference spectra at 1540 and 1450 cm^{-1}, respectively, by extinction coefficients reported by Emeis.[21]

Thermal gravimetric (TG) analysis of deactivated catalysts was conducted on an SDT-Q600instrument (TA, USA). In a typical TG experiment, about 20 mg sample was pre-treated with N_2 (100mL/min) at 473 K for 1 h to remove the adsorbed moisture in the catalyst sample. After cooling to room temperature in N_2, the sample was heated to 1073 K in an air flow (100 mL/min) at a heating rate of 10 K/min.

Organic species trapped in the channels of mordenite zeolites during reactions were analyzed following the procedures as described in the literature.[22] Spent catalysts were dissolved in 20% hydrofluoric acid solution. Organic phase was extracted by dichloromethane (CH_2Cl_2) and then analyzed using an Agilent 7890A/5975C GC/MSD.

2.3. Catalysts test

DME carbonylation experiments were performed in a continuous flow fixed-bed stainless steel reactor. 1.0 g catalyst (40–60 mesh) was packed in the reactor and pretreated in N_2 at 673K for 2h. After the catalyst sample cooling to 473 K, reactant gas mixture(5% DME,35% CO, and 60% H_2) was introduced into the reactor at a gas hourly space velocity (GHSV) of 1500 mL/(g·h). Reaction pressure was 3.0MPa. The outlet gas was analyzed online using a gas chromatograph (Agilent 7890A) equipped with TCD and FID detectors.

3. Results and Discussion

3.1. Structure analysis

XRD patterns of Fe-modified HMOR samples with various iron contents are shown in Fig.1 and Table 1. The typical diffraction peaks of mordenite-type zeolites are clearly observed for the four samples without any other crystalline diffraction peaks. As shown from the diffraction patterns in Fig. S1, it is obvious that

the peaks shift to the lower frequencies with the increase of iron content, indicating the increase of d values, the basal spacing. It is the prominent proof that the larger Fe^{3+} (0.63 Å) was introduced in the mordenite framework in replace of the smaller

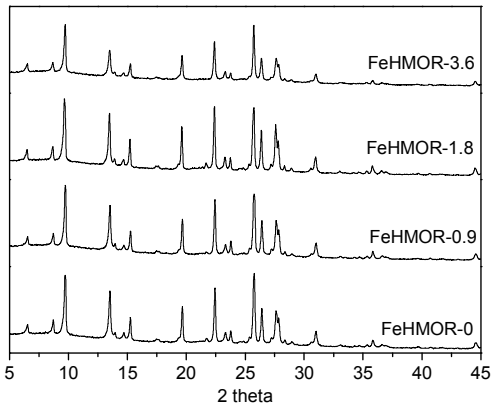

Fig.1. X-ray diffractions of FeHMOR samples

Al^{3+} (0.53 Å).[23] The relative crystallinities of the samples were calculated according to the area sum of the seven strong peaks between 5 and 30° of 2θ, assuming the relative crystallinity of FeHMOR-0 zeolite was 100%. The comparison of 96% and 104% relative crystallinities of FeHMOR-0.9 and FeHMOR-1.8 with the 100% relative crystallinity of FeHMOR-0 indicated that the two samples were in good crystal state after introduction of the iron but the 56% relative crystallinity of FeHMOR-3.6 showed that the framework of mordenite collapsed to some extent as the iron content increase from 0 to 3.6%. As summarized in Table 1, the iron element content measured by XRF are about 0.04, 0.89, 1.62 and 3.05wt% respectively and were in accordance with those of the designed contents.

The substitution of Fe for Al and the increased of iron content resulted in the IR framework bands losing the sharpness progressively and shifting to lower wavenumbers, as shown in Fig.S2. The most sensitive band to the substitution was the

Table 1 Relative crystallinities and iron content of FeHMOR samples

	Relative Crystallinity	Si/(Al+Fe) (XRF)	Iron Content wt% (XRF)
FeHMOR-0	100%	7.5	0.04
FeHMOR-0.9	96%	7.2	0.89
FeHMOR-1.8	104%	7.1	1.62
FeHMOR-3.6	56%	6.6	3.05

internal asymmetric stretching vibration of Si-O-T observed at 1084cm^{-1} for aluminosilicate.[23] The differences of this band between the four samples indicated that Fe was already in the framework of Fe-modified HMOR samples.[23] The information from the Fig.S2 is consistent with the results of XRD above and further confirms the existence of Fe in the framework of mordenites.

Fig.S3 shows the UV-Vis reflectance spectra measured with FeNaMOR samples containing different content of iron at room temperature. Two common features are observed in the spectra of Fe-modified mordenites, the strong absorption bands in the 200~300 nm interval due to the charge transfer from ligand to isolated framework Fe^{3+} ions, and the weak bands in the range of 370~450 nm related to d-d transitions of Fe^{3+} ions in tetrahedral symmetry.[23-26] Therefore, Fe in the modified Na-mordenites was dominated by tetrahedral Fe^{3+} ions.

UV resonance Raman spectroscopy is a unique, practical and powerful technique to detect the isolated transition metal atoms in the framework of zeolites.[27-29] The laser line 244 nm was used as the excitation source because it was near the charge transfer bands at 230 nm. In the resonance Raman spectra of the transition metal substituted zeolites, the observed bands at about 500 and 1100 cm^{-1} could be taken as the characteristic bands for the presence of the transition metal ions in tetrahedral coordination in the framework sites of zeolites[28].

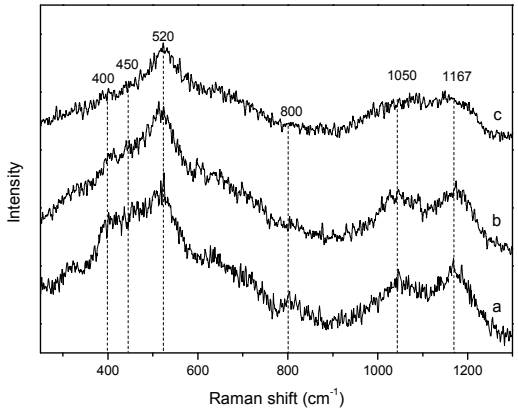

Fig.2. UV resonance Raman spectra of FeHMOR samples
a: FeHMOR-0.9, b: FeHMOR-1.8, c: FeHMOR-3.6

UV resonance Raman spectra of FeHMOR samples with various iron contents excited by 244 nm excitation line are shown in Fig. 2. The bands centered at about 400, 450, 800 cm^{-1} are the characteristic bands of MOR structure[30]. The bands at 520 and 1050 cm^{-1} are the resonance Raman bands associated with the isolated iron species in the framework, due to the Fe-O-Si symmetric and asymmetric stretching mode of the isolated tetrahedral iron ions in the silica framework, respectively.[28, 31] As in the report about UV Raman spectra of the Fe-ZSM-5[29], the band at 1165 cm^{-1} is related to the framework crystallinity of the zeolite. The appearance of this band in Fig. 2 for the FeHMOR-0.9 and FeHMOR-1.8 indicated that the iron atoms were tightly coordinated in the framework of FeHMOR. However, the remarkable decrease in the intensity of the band for the sample FeHMOR-3.6 illustrated that the crystal state was poor and the partial iron dropped from the framework. The similar result was also observed from the relative crystallinity in Table 1.

The ion exchange from Na to H induced clear modification in the UV-Vis spectra, a new peak at about 275 nm and almost disappearance of d-d region. These results were confirmed by UV-Vis spectra of FeHMOR samples in Fig. 3 and the difference spectrum (FeHMOR-FeNaMOR) in Fig.S4. According to the literature, the strong charge transfer absorption at about 277 nm represents the Fe^{3+} species in octahedral complexes, and the broad absorption at about 330 nm reveals the presence of octahedral Fe^{3+} present in small clusters, such as observed for clustered Fe^{3+} in hydroxides.[24] As shown in Fig.3, the decrease of 230 nm and increase of 275 nm suggested that the process of ion exchange from Na to H, including ion exchange, drying and calcination, resulted in partial tetrahedral Fe^{3+} dropping from framework and forming the extra-framework octahedral iron species. The peaks in the different spectrum Fig.S4 indicated that some extra-framework

Fe^{3+} species may be in octahedral complexes and some in small clusters. The color of the FeNaMOR zeolites was completely white, indicating the absence of colored oxides of iron in bulk. But the Fe-containing HMORs were light brown in color, typical of samples containing iron oxides and hydroxide.[32, 33] The diffraction peaks ascribing to the iron oxides were not found in the XRD spectra of the four Fe-HMORs after careful comparison and match. The iron oxides may be highly dispersed in the samples.

N_2 adsorption curves of all four samples with or without Fe exhibit type I curves (Fig.S5), the typical N_2 adsorption-desorption isotherms for microporous materials. The corresponding pore volumes and BET surface areas are summarized in Table 2. Comparing the pore volume and micropore volume, the BET surface and micropore area, FeHMOR zeolites also proved to be microporous materials. The decrease of nitrogen uptake was observed for the sample FeHMOR-3.6, which was possibly attributed to the blocking or filling of micropores by extra-framework species or the low relative crystallinity.

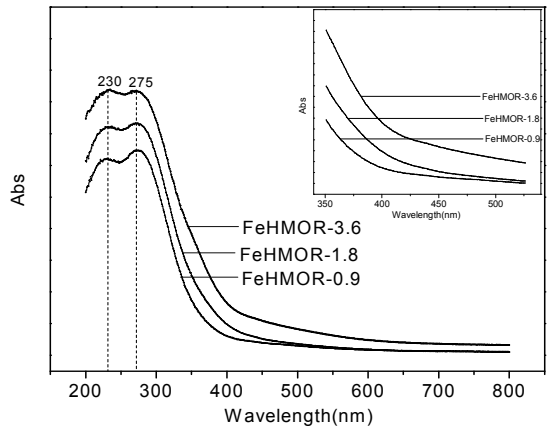

Fig.3.UV-Vis spectra of FeHMOR samples

Table 2 Textural property of zeolites with different iron content

	FeHMOR -0	FeHMOR-0.9	FeHMOR -1.8	FeHMOR -3.6
PoreVolume (cm^3/g)	0.201	0.210	0.200	0.184
Micropore Volume (t-plot, cm^3/g)	0.171	0.177	0.176	0.163
BET surface area (m^2/g)	399	417	403	320
Micropore area (t-plot, cm^3/g)	367	382	377	292

3.2. Catalytic performance

Changes in DME conversion and MAc selectivity with time-on-stream (TOS) for all four catalysts are shown in Fig. 4. The reaction conditions, including reaction temperature, pressure, gas space velocity and feed composition, were almost the same and thus the obtained DME conversion was indicative of the corresponding catalyst activities in the four tests. Catalysts activities in all experiments initially increased with time and reached the maximum values of DME conversion, and then began to decline with increase in time. Obviously, FeHMOR-0.9 had the highest activity (85%) and was higher than the FeHMOR-0 catalyst (75%), whereas the FeHMOR-3.6 catalyst was the least active (about 40% DME conversion). With the increase of iron content from 0.0 to 3.6%, the maximum value of catalyst activity among four tests was obtained by FeHMOR-0.9, not by FeHMOR-3.6 or FeHMOR-0. This result was consistent with the changing trend of the BET surface areas and pore volumes, implying the close relation between them during the carbonylation reaction of DME. Detailed research is required to verify the validity of this hypothesis. Also, the corresponding stabilities for all four catalysts had obvious improvement, as shown in Fig. 4b. In addition, the induction periods of all four catalysts prolonged from 2 to 5 h with the increase of iron content. It was obvious that an appropriate amount of iron in the framework of mordenite catalyst favored the catalytic performance of DME carbonylation catalysts.

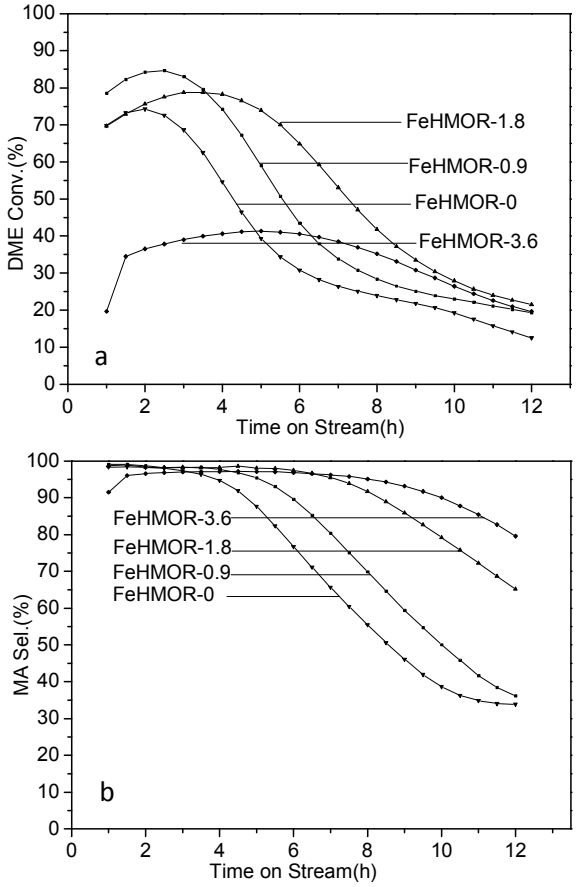

Fig.4. DME conversion of (a) and MAc selectivity (b) of DME carbonylation over Fe-modified HMOR catalysts Reaction conditions: 473K, 3.0 MPa, 5%DME, 35%CO, and 60%H_2

3.3. Analysis of cokes retained in deactivated catalysts

Cokes in the four deactivated catalysts after DME carbonylation reactions for 12 h at 473 K and 3MPa were characterized by TG analysis and the results are shown in Fig. 5a and 5b. All four profiles show two distinct weightlessness peaks in Fig.5b. The first peak at low temperature was likely attributed to the combustion of soft coke like reaction intermediates, such as surface bound methyl and acetyl associated with the formation of MAc, and the second peak at high temperature might be assigned to the removal of heavy

coke formed during the reaction.[7, 34, 35] Fig.5b shows the combustion temperatures of coke in DTG. It can be found that the combustion temperatures of heavy coke are different significantly from each other, 843, 803, 748, and 742K for FeHMOR-0, FeHMOR-0.9, FeHMOR-1.8 and FeHMOR-3.6 respectively, decreasing with the increase of iron content in the catalysts. The same tendency was obtained for the combustion temperature of the soft coke. The difference in combustion temperature of hard and soft coke demonstrated that the composition of coke was different in the four samples and the coke molecules were lighter as the increase of iron content.

The weight loss of the deactivated FeHMOR-0 catalyst is 10.58wt%, 81 percent hard coke and 19 percent soft coke. Whereas the deactivated FeHMOR-1.8 has 10.81 wt% cokes with 66% hard coke and 34% soft coke. As the iron amount increasing to 3.6wt%, however, the hard coke and soft coke in the used FeHMOR-3.6 are 45% and 55% respectively with the coke amount of 7.02 wt%, much less than that in the used FeHMOR-0 catalyst. Therefore the reactions of coke formation and transforming soft coke into hard coke were suppressed effectively due to the introduction of iron.

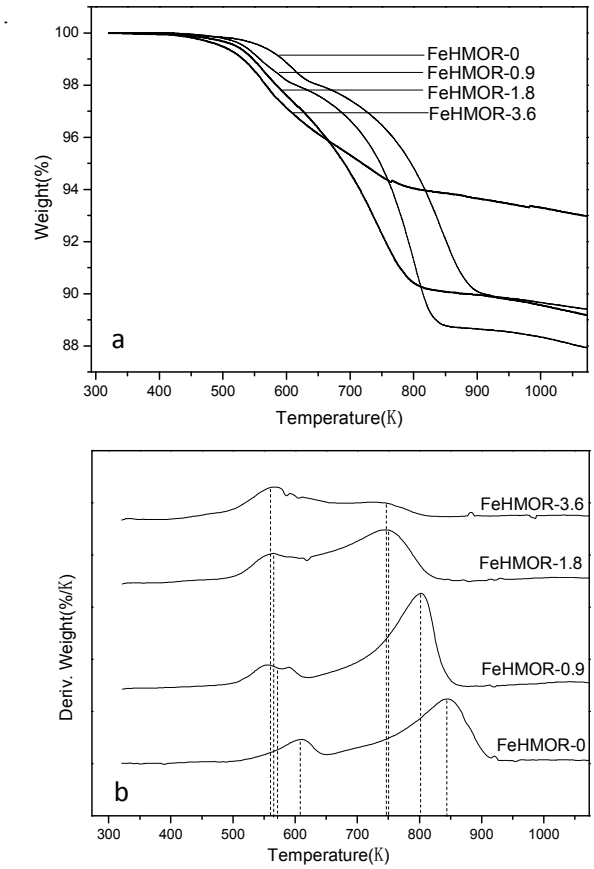

Fig.5. Thermal analysis of coke in deactivated catalysts (a:TG;b:DTG)

After 12 h of DME carbonylation reaction at 473 K and 3MPa, the deactivated catalysts were dissolved in HF and the compositions of chemical compounds in it are described in detail in Fig. S6. The structures on the chromatograms are peak identifications by comparison with the NIST database, and the asterisk (*) represents the internal standard (C_2Cl_6). The adamantane species and methylbenzene species, mainly before retention time 25 min, were detected in all spent catalysts. And the species after retention time 25 min were mainly the bulky polycyclic aromatics. Some higher molecular weight chemical compounds were also detected. The amounts of polycyclic aromatics confined in FeHMOR-0 after 25 min of the retention time are obviously more than these in FeHMOR-1.8 and FeHMOR-3.6. The relative lower density of organic species meant the slighter coke deposition during DME conversion, indicating that Fe in mordenite zeolites can effectively inhibit carbon deposition, which was also confirmed by TG analysis.

As a competitive reaction of DME carbonylation to MAc, DME to olefins reaction forms adamantane species and methylbenzenes species, the important intermediates for the formation of heavy hydrocarbons.[36] Accommodation of large hydrocarbon species in the channels of zeolite catalysts causes the great limitation in mass transfer of reactants and products. When a significant fraction of the 12MR channels of mordenites is occupied by heavy hydrocarbons, catalysts start to deactivate with decrease in DME conversion and MAc selectivity.

3.4. Characterization of acid sites in 12MR channels of mordenite

DME adsorbed on acid sites in the 12MR channels of mordenite could convert into olefins which cause the formation of heavy hydrocarbons through oligomerization and hydride transfer reaction. The intersection between 12MR channels and 8MR channels would be blocked if the amount of heavy hydrocarbons is enough, which leads to the diffusion pathway inefficient for reactants and products.[7, 37] Therefore, removing and/or neutralizing and/or weakening acid sites in 12MR channels would be an effective method to improve the stability of MOR catalysts while keeping a high MAc activity.

The T2 and T4 sites in the 12MR channel were the two energetically preferred positions for Fe substitution in the MOR framework, as shown in Fig. S7.[38] The acid sites, with Fe in the framework of zeolites, are much less active and do not readily catalyze hydride-transfer reactions, thus exhibit a much lower tendency to form coke during reactions of olefins.[39] Therefore, it is supposed that the partial introduction of Fe in place of Al in the framework would suppress the coke formation reaction to some extent. Understanding of the concentration and strength of acid sites in zeolites would provide illustration to the reaction results and the coke composition retained in the catalysts.

FT-IR and solid state NMR spectroscopic techniques by adsorbing basic probe molecules have been widely used to characterize acid sites in zeolites and other solid catalysts.

The size of TMPO (kinetic diameter ca. 0.55 nm) and pyridine (kinetic diameter: 0.585 nm) are slightly smaller than that of the 12-MR channels (0.67×0.70 nm) of mordenite, but much larger than that of the 8-MR channels (0.28×0.57 nm). TMPO and pyridine would selectively adsorb on the acidic sites located in the 12-MR channels.[7, 40] Therefore the ^{31}P MAS NMR of adsorbed TMPO has been used to probe surface acidity, as the ^{31}P chemical shift of TMPO is sensitive to acid strength.[41-43] And the amount of acid sites in the 12MR channel was characterized by the FTIR after adsorption of pyridine.

Fig. S8 displays ^{31}P MAS NMR spectra of the TMPO-adsorbed samples. The signals between 80 and 50 ppm were ascribed to TMPO adsorbed on Brønsted acid sites or chemisorbed species.[40] The intense signal at 46 ppm was ascribed to physisorbed or weakly adsorbed TMPO. The solid TMPO

contributed to the resonance at ~39 ppm.[41] The higher chemical shift of ^{31}P reveals the stronger acid strength.
All the four spectra reveal similar feature, and can be deconvoluted into three characteristic resonances by Gaussian simulation. The deconvolution results and relative area ratios for different sites are shown in Table 3.

Table 3 Distributions of Brønsted acid sites of various catalysts detected by ^{31}P MAS NMR using TMPO probe molecule

	Site I ~82 ppm Area (%)	Site II ~67 ppm Area (%)	Site III ~51 ppm Area (%)
FeHMOR-0	4.81	39.99	55.20
FeHMOR-0.9	4.65	42.39	52.96
FeHMOR-1.8	1.93	36.37	61.71
FeHMOR-3.6	1.98	35.13	62.89

It is well-known that the higher chemical shift of ^{31}P value represents the stronger acid strength. Thus acid sites with the chemical shift at the site I was identified as strong acid sites, the site II the moderate acid sites and the site III the weak acid sites. As shown in Table 3, the proportions of strong and moderate acid sites decreased and the weak acid sites increased correspondingly as the iron content increased from 0.0 to 3.6wt%. The more percent of acid sites with the less acid strength would depress the tendency of coke formation. Therefore, the decline of acid strength resulted in the decrease of coke retained in catalysts after introduction of iron atoms.

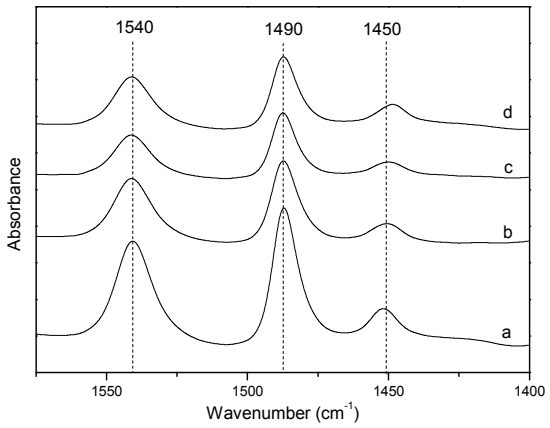

Fig. 6 Pyridine-IR spectra of the FeHMOR samples: a: FeHMOR-0; b: FeHMOR-0.9; c: FeHMOR-1.8; d: FeHMOR-3.6.

Pyridine-IR measurements were performed to investigate the acid density mainly in the 12MR channels of mordenite; the results are shown in Fig. 6. In general, the two adsorption peaks appeared at ~1450 and 1540 cm^{-1} corresponding to the characteristic vibration peaks of pyridine molecules adsorbed on Lewis and Brönsted acid sites, forming PyL (pyridine bonded to Lewis sites) and Py^{+} (pyridinium ions), respectively.[44] The adsorption peak at around 1490 was usually classified as Brönsted and Lewis acid sites.
The concentrations of Brønsted and Lewis acid sites of the FeHMOR samples calculated from IA area of the bands at about 1540 and 1450 cm^{-1} according to the extinction coefficients reported by Emeis.[21] The calculation results are shown in Fig. 7. The concentration of acid sites which would adsorb pyridine molecules at 573K decreased from 0.23 to 0.12 mmol/g when the iron content increases from 0.0 to 3.6wt%. As a consequence, the oligomerization and hydride

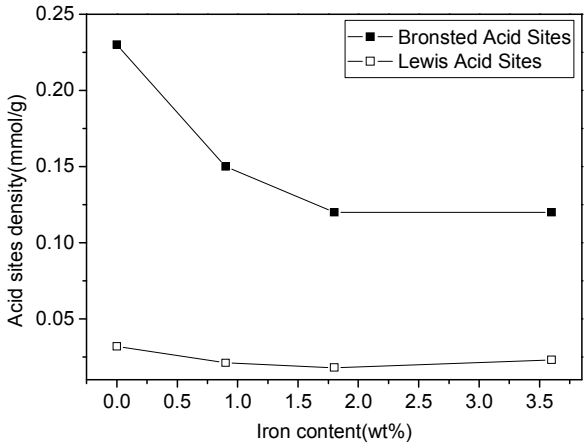

Fig.7.The quantitative calculation of Brønsted and Lewis acid sites mainly in 12MR channels of mordenite

reactions leading to the formation of coke were effectively suppressed,[39] which can be demonstrated by the decrease of the coke amount and the combustion temperature as the increase of iron content in the catalysts shown in Fig. 5. Therefore, the stability of FeHMOR catalysts during the tests of DME carbonylation improved, as shown in Fig. 4b.

Conclusions

In this study, a series of mordenite samples with the iron content from 0.0 to 3.6wt% in zeolite were synthesized by a template-free method and employed in DME carbonylation reaction. Fe atoms were introduced into the framework of mordenite zeolite and the acid strength and density in 12MR channels of mordenite were found to be reduced after the introduction of Fe in the zeolite framework, which were evident by the characterization results of ^{31}P MAS NMR and FTIR. As a consequence, the performance of FeHMOR samples was markedly improved. With the increase of iron content from 0.0 to 3.6wt%, DME conversion increased and then decreased. Also, the corresponding stabilities for all four catalysts still kept growing. These results were due to the inhibition of coke formation in the 12MR channels of mordenite during DME carbonylation reaction. The corresponding amount of coke in the used catalysts was reduced with the increase of iron content. And the deposited chemical compounds on catalysts were primarily adamantane species, methylbenzenes and polycyclic aromatic. Results achieved in this study with iron modified mordenite catalysts are encouraging, and further studies on the improvement of performance are required.

Acknowledgements

We acknowledge the financial support from the National Natural Science Foundation of China (Grant No. 21473182, 21303106).

Notes and references

[a]National Engineering Laboratory for Methanol to Olefins, Dalian Institute of Chemical Physics, Chinese Academy of Sciences, P. O. Box 110, 116023 Dalian, PR China

[b]Dalian National Laboratory for Clean Energy, Dalian Institute of Chemical Physics, Chinese Academy of Sciences, Dalian, PR China

[c]Graduate University of Chinese Academy of Sciences, Beijing 100049, PR China

* Corresponding authors at: National Engineering Laboratory for Methanol to Olefins, Dalian Institute of Chemical Physics, Chinese Academy of Sciences, P. O. Box 110, 116023 Dalian, PR China. Tel. /fax: +86 0411 84379518.E-mail addresses: liuzm@dicp.ac.cn (Z. Liu)

Electronic Supplementary Information (ESI) available: [details of any supplementary information available should be included here]. See DOI: 10.1039/b000000x/

1. K. Fujimoto, T. Shikada, K. Omata and H. Tominaga, *Chem. Lett.*, 1984, 2047-2050.
2. A. Bhan, A. D. Allian, G. J. Sunley, D. J. Law and E. Iglesia, *J. Am. Chem. Soc.*, 2007, **129**, 4919-4924.
3. P. Cheung, A. Bhan, G. J. Sunley and E. Iglesia, *Angew Chem Int Ed Engl*, 2006, **45**, 1617-1620.
4. P. Cheung, A. Bhan, G. Sunley, D. Law and E. Iglesia, *J. Catal.*, 2007, **245**, 110-123.
5. M. Boronat, C. Martinez-Sanchez, D. Law and A. Corma, *J. Am. Chem. Soc.*, 2008, **130**, 16316-16323.
6. B. Li, J. Xu, B. Han, X. Wang, G. Qi, Z. Zhang, C. Wang and F. Deng, *The Journal of Physical Chemistry C*, 2013, **117**, 5840-5847.
7. J. Liu, H. Xue, X. Huang, P. Wu, S. Huang, S. Liu and W. Shen, *Chin. J. Catal.*, 2010, **31**, 729-738.
8. H. Xue, X. Huang, E. Zhan, M. Ma and W. Shen, *Catal. Commun.*, 2013, **37**, 75-79.
9. M. D. Jones, C. G. Keir, C. D. Iulio, R. A. M. Robertson, C. V. Williams and D. C. Apperley, *Catal. Sci. Technol.*, 2011, **1**, 267-272.
10. R. N. Singh and R. Awasthi, *Catal. Sci. Technol.*, 2011, **1**, 778-783.
11. R. K. Niven, *Renew. Sust. Energ. Rev.*, 2005, **9**, 535-555.
12. P. D. Vaidya and A. E. Rodrigues, *Chem. Eng. J.*, 2006, **117**, 39-49.
13. A. C. Hansen, Q. Zhang and P. W. Lyne, *Bioresour. Technol.*, 2005, **96**, 277-285.
14. X. G. San, Y. Zhang, W. J. Shen and N. Tsubaki, *Energy Fuels*, 2009, **23**, 2843-2844.
15. M. Hartmann and L. Kevan, *Chem. Rev.*, 1999, **99**, 635-664.
16. B. Ellis, M. J. Howard, R. W. Joyner, K. N. Reddy, M. B. Padley and W. J. Smith, *11th International Congress on Catalysis - 40th Anniversary, Pts a and B*, 1996, **101**, 771-779.
17. T. Blasco, M. Boronat, P. Concepcion, A. Corma, D. Law and J. A. Vidal-Moya, *Angew. Chem.-Int. Edit.*, 2007, **46**, 3938-3941.
18. X. Zhang, Y. P. Li, S. B. Qiu, T. J. Wang, M. Y. Ding, Q. Zhang, L. L. Ma and Y. X. Yu, *Chin. J. Chem. Phys.*, 2013, **26**, 77-82.
19. V. I. Sobolev, G. I. Panov, A. S. Kharitonov, V. N. Romannikov, A. M. Volodin and K. G. Ione, *J. Catal.*, 1993, **139**, 435-443.
20. M. A. Uddin, T. Komatsu and T. Yashima, *J. Catal.*, 1994, **150**, 439-441.
21. C. A. Emeis, *J. Catal.*, 1993, **141**, 347-354.
22. M. Guisnet, L. Costa and F. R. Ribeiro, *J. Mol. Catal. A-Chem.*, 2009, **305**, 69-83.
23. P. Wu, T. Komatsu and T. Yashima, *Microporous Mesoporous Mat.*, 1998, **20**, 139-147.
24. S. Bordiga, R. Buzzoni, F. Geobaldo, C. Lamberti, E. Giamello, A. Zecchina, G. Leofanti, G. Petrini, G. Tozzola and G. Vlaic, *J. Catal.*, 1996, **158**, 486-501.
25. T. Inui, H. Nagata, T. Takeguchi, S. Iwamoto, H. Matsuda and M. Inoue, *J. Catal.*, 1993, **139**, 482-489.
26. P. Ratnasamy and R. Kumar, *Catal. Today*, 1991, **9**, 329-416.
27. C. Li, G. Xiong, J. Liu, P. Ying, Q. Xin and Z. Feng, *J. Phys. Chem. B*, 2001, **105**, 2993-2997.
28. K. Sun, F. Fan, H. Xia, Z. Feng, W.-X. Li and C. Li, *J. Phys. Chem. C*, 2008, **112**, 16036-16041.
29. F. Fan, K. Sun, Z. Feng, H. Xia, B. Han, Y. Lian, P. Ying and C. Li, *Chem.-Eur. J.*, 2009, **15**, 3268-3276.
30. J. Wang, H. Xia, X. Ju, F. Fan, Z. Feng and C. Li, *Chin. J. Catal.*, 2013, **34**, 876-888.
31. H. Xin, J. Liu, F. Fan, Z. Feng, G. Jia, Q. Yang and C. Li, *Microporous Mesoporous Mat.*, 2008, **113**, 231-239.
32. A. Meagher, V. Nair and R. Szostak, *Zeolites*, 1988, **8**, 3-11.
33. J. Perez-Ramirez, F. Kapteijn and A. Bruckner, *J. Catal.*, 2003, **218**, 234-238.
34. M. Guisnet and P. Magnoux, *Appl. Catal. A-Gen.*, 2001, **212**, 83-96.
35. L. Palumbo, F. Bonino, P. Beato, M. Bjorgen, A. Zecchina and S. Bordiga, *J. Phys. Chem. C*, 2008, **112**, 9710-9716.
36. H. Xue, X. Huang, E. Ditzel, E. Zhan, M. Ma and W. Shen, *Ind. Eng. Chem. Res.*, 2013, **52**, 11510-11515.
37. B. Li, J. Xu, B. Han, X. Wang, G. Qi, Z. Zhang, C. Wang and F. Deng, *J. Phys. Chem. C*, 2013, **117**, 5840-5847.
38. S. P. Yuan, J. G. Wang, Y. W. Lia and H. J. Jiao, *Theochem-J. Mol. Struct.*, 2004, **674**, 267-274.
39. O. Kresnawahjuesa, *J. Catal.*, 2002, **210**, 106-115.
40. A. Zheng, B. Han, B. Li, S. B. Liu and F. Deng, *Chem. Commun.*, 2012, **48**, 6936-6938.
41. S. Hayashi and N. Kojima, *Microporous Mesoporous Mat.*, 2011, **141**, 49-55.
42. A. Zheng, H. Zhang, X. Lu, S. B. Liu and F. Deng, *J. Phys. Chem. B*, 2008, **112**, 4496-4505.
43. A. Zheng, S. J. Huang, S. B. Liu and F. Deng, *Phys. Chem. Chem. Phys.*, 2011, **13**, 14889-14901.
44. P. Ayrault, J. Datka, S. Laforge, D. Martin and M. Guisnet, *J. Phys. Chem. B*, 2004, **108**, 13755-13763.

Graphical Abstract

Promotion Effect of Fe in Mordenite Zeolite on Carbonylation of Dimethyl Ether to Methyl Acetate

Hui Zhou[a,b,c], Wenliang Zhu[a,b], Lei Shi[a,b], Hongchao Liu[a,b], Shiping Liu[a,b,c], Shutao Xu[a,b], Youming Ni[a,b], Yong Liu[a,b], Lina, Li[a,b,c], Zhongmin Liu[*a,b]

[a]National Engineering Laboratory for Methanol to Olefins, Dalian Institute of Chemical Physics, Chinese Academy of Sciences, P. O. Box 110, 116023 Dalian, PR China

[b]Dalian National Laboratory for Clean Energy, Dalian Institute of Chemical Physics, Chinese Academy of Sciences, Dalian, PR China

[c]Graduate University of Chinese Academy of Sciences, Beijing 100049, PR China

*E-mail addresses: liuzm@dicp.ac.cn (Z. Liu)

Fe-modified mordenite samples were synthesized and employed in dimethyl ether carbonylation reaction, resulting in an evident improvement on the stability.